WATER RESOURCES RESEARCH, VOL. 34, NO. 10, PAGES 2655–2670, OCTOBER 1998

On the simulation of infiltration- and saturation-excess runoff using radar-based rainfall estimates: Effects of algorithm uncertainty and pixel aggregation

Michael Winchell,[1] Hoshin Vijai Gupta, and Soroosh Sorooshian
Department of Hydrology and Water Resources, University of Arizona, Tucson

Abstract. The effects of uncertainty in radar-estimated precipitation input on simulated runoff generation from a medium-sized (100-km^2) basin in northern Texas are investigated. The radar-estimated rainfall was derived from Next Generation Weather Radar (NEXRAD) Level II base reflectivity data and was supplemented by ground-based rain-gauge data. Two types of uncertainty in the precipitation estimates are considered: (1) those arising from the transformation of reflectivity to rainfall rate and (2) those due to the spatial and temporal representation of the "true" rainfall field. The study explicitly differentiates between the response of simulated saturation-excess runoff and infiltration-excess runoff to these uncertainties. The results indicate that infiltration-excess runoff generation is much more sensitive than saturation-excess runoff generation to both types of precipitation uncertainty. Furthermore, significant reductions in infiltration-excess runoff volume occur when the temporal and spatial resolution of the precipitation input is decreased. A method is developed to relate this storm-dependent reduction in runoff volume to the spatial heterogeneity of the highest-intensity rainfall periods during a storm.

1. Introduction

The past decade has marked a new era in the field of hydrology, resulting from the installation of the U.S. National Weather Service Next Generation Weather Radar (NEXRAD) network [*Klazura and Imy*, 1993]. This network of WSR-88D Doppler radars has not only revolutionized modern meteorological forecasting but also promises to improve hydrological forecasting. The primary contribution of the radar to hydrology is the high spatial and temporal resolution and large areal coverage of the precipitation products which are generated. These products provide detailed information on precipitation events, previously unattainable with simple networks of ground-based rain gauges. The benefits of having quantitative rainfall information over large areas with a high temporal and spatial resolution have applications in all aspects of hydrology and water resources management [see *Cluckie*, 1991]. *Cluckie* [1991] emphasized that in order for weather radar to reach its potential in hydrology, high-quality radars capable of producing products at a small spatial and temporal scale will be necessary. This task is far from trivial as expressed by the work of numerous authors who have spent many years addressing the problem [*Collier*, 1986a, b; *Tees and Austin*, 1991; *Kitchen and Blackall*, 1992; *Seo et al.*, 1995; *Smith et al.*, 1996a]. While continuing to improve techniques for estimating rainfall from radar, these authors acknowledge that a great deal of uncertainty in the quality of the estimates still exists. In the meantime, many studies have focused on the application of radar-estimated precipitation in flood-forecasting applications [*Kouwen and Garland*, 1989; *Schell et al.*, 1992; *James et al.*, 1993; *Becchi et al.*, 1994; *Mimikou and Baltas*, 1996]. Unfortunately, meaningful hydrologic predictions are not possible unless the uncertainty associated with the radar-derived precipitation can be quantified and corrected for. The uncertainty in rainfall estimation from radar reflectivity may be separated into two broad categories: (1) errors resulting from the transformation of reflectivity to rainfall and (2) errors due to the spatial and temporal representation of the true rainfall field.

There has not been a consensus as to the effects of uncertainty in the transformation of reflectivity to rainfall on runoff modeling, nor has the topic received substantial attention. *Wyss et al.* [1990] suggested that errors in runoff predictions due to errors in the radar-estimated rainfall input are of less significance than the errors introduced in the conversion from rainfall to runoff. This is contradictory to the conclusions of *Numec* [1985] and *Hudlow et al.* [1983], who argued that errors in precipitation input to a rainfall-runoff model will result in substantial errors in simulated runoff. *Collier and Knowles* [1986] indicated that specific circumstances exist where errors in precipitation input to a rainfall-runoff model will be dampened in the conversion to runoff and other circumstances where the precipitation errors will be magnified in the conversion to runoff. While the above cited studies address the effects of rainfall errors on runoff simulations, the authors of this paper are aware of only one publication which has investigated how hydrologic predictions are affected by changes in the parameters of the reflectivity to rainfall transformation. In that paper, *Pessoa et al.* [1993] found that different widely accepted reflectivity-rainfall (Z-R) relationships resulted in significantly different simulated hydrographs. The paper suggests that identification of appropriate Z-R relationship parameters in real time is necessary in order to produce reliable hydrologic forecasts with radar-estimated precipitation. In the use of historical radar data for hydrologic simulations, there are many options available for the identification of proper Z-R parameters and subsequent precipitation bias correction.

[1]Now at Northeast River Forecast Center, National Weather Service, Taunton, Massachusetts.

Paper number 98WR02009.
0043-1397/98/98WR-02009$09.00

An investigation into the effects of employing different strategies for Z-R parameter identification on hydrologic simulations is still needed.

Considerably more attention has been given to studying the effects of uncertainty in precipitation input, due to its spatial and temporal representation, on runoff simulations. The conclusions have been that runoff generation is highly sensitive to the spatial and temporal scale of the input [*Milly and Eagleson*, 1988; *Loague*, 1988; *Kouwen and Garland*, 1989; *Krajewski et al.*, 1991; *Ogden and Julien*, 1993, 1994; *Michaud and Sorooshian*, 1994; *Faures et al.*, 1995; *Shah et al.*, 1996]. Several of these studies found that runoff volumes increase as the heterogeneity of the rainfall field becomes better represented [*Milly and Eagleson*, 1988; *Kouwen and Garland*, 1989; *Michaud and Sorooshian*, 1994], while one study [*Faures et al.*, 1995] found a general reduction in runoff volumes as the heterogeneity in the rainfall becomes better represented. In addition, *Obled et al.* [1994] found that while runoff simulations were quite sensitive to the spatial scale of the precipitation input, they were not sensitive to the temporal representation of the precipitation. This finding contradicts a primary conclusion of *Krajewski et al.* [1991] that representation of the temporal variability of the rainfall is more important than properly representing the spatial variability. One possible explanation to the apparent discrepancy in these conclusions is the difference in the rainfall-runoff models employed. In the study by *Obled et al.* [1994], saturation-excess runoff was modeled by the TOPMODEL approach, while *Krajewski et al.* [1991] modeled the infiltration-excess runoff mechanism with a modified Soil Conservation Service curve number method. *Loague* [1988] actually simulated both types of runoff generation, showing significant differences in their response to precipitation variability. Looking more closely at the other past studies which examined runoff sensitivity to precipitation scale, all of those cited happened to use the infiltration-excess mechanism to model the runoff generation.

A review of these past studies suggests that there has been a bias toward the use of infiltration-excess type runoff as opposed to the saturation-excess type in the investigations into precipitation scale effects on runoff simulations. The few studies which have investigated the saturation-excess mechanism provided evidence that generalizations concerning the effects of rainfall variability on runoff generation cannot be made. *Shah et al.* [1996] recognized this when they suggested that to understand why averaging of rainfall produces larger errors in runoff for some storms than others requires that an investigation into the active runoff-generation mechanisms be performed.

Several questions related to the use of radar data for rainfall-runoff modeling remain unresolved, including (1) how significantly will errors in the precipitation data, due to the transformation of reflectivity to rainfall, affect runoff simulations, (2) how significantly will the aggregation of the radar product in time and space affect runoff simulations, and (3) do differently modeled surface-runoff mechanisms (infiltration-excess and saturation-excess) respond differently to these sources of precipitation uncertainty? This paper addresses these questions through application of radar-estimated precipitation to a distributed rainfall-runoff model for a medium-sized watershed in northern Texas.

Table 1. Storm Events Studied and Location of Radar Data

Storm Date	Origin of Radar Data
Oct. 28, 1991	Twin Lakes (KTLX)
Oct. 31, 1991	Twin Lakes (KTLX)
Sept. 10, 1992	Frederick (KFDR)
Feb. 24, 1993	Twin Lakes (KTLX)
May 9, 1993	Frederick (KFDR)
May 12, 1994	Twin Lakes (KTLX)
April 10, 1995	Twin Lakes (KTLX)

2. Background Information

2.1. Study Site

The region chosen for this study was the southern plains of the United States. The climate of this region in north central Texas near Gainesville is dominated by frontal precipitation associated with large synoptic scale low-pressure systems during the fall and winter, with intense convective activity during the spring and early summer. Accordingly, rainfall is uniformly distributed throughout the year, with a slight maximum during the spring. Snow is infrequent. The physical highlights of this region are the Red River and Lake Texoma to the north and the broad-sloping plains and gently rolling hills which cover the region.

The Timber Creek watershed was chosen for this study because of minimal flow regulation, its size (102 km^2) and susceptibility to flash floods, and the occurrence of several large floods during the period of radar data availability. The watershed is oriented primarily north to south and varies in elevation from 282 m at the hilltops of the headwaters to 198 m at the watershed outlet. Timber Creek consists primarily of pasture, with small areas of woodlands and numerous agricultural stock ponds. Watershed soils are primarily sandy loam and loamy sand, with small areas of loam and loamy clay. The main channel length of Timber Creek is 22.9 km, with an average slope of 0.0025. In most years, Timber Creek is a perennial stream with very low flows during August and September; however, in some years it dries up for a few weeks during those months. The peak flow of record (since 1985) for Timber Creek is 376.4 m^3/s.

2.2. Description of Data

One reason for choosing north central Texas for this study was the relatively long period of radar data covering the region. Twin Lakes, Oklahoma, is the site of the first radar to begin operation and, accordingly, has the longest record of data. Along with data from the Twin Lakes, Oklahoma, radar (KTLX), data from Frederick, Oklahoma (KFDR), were also used in this study. An effort was made to obtain the largest storms with a complete radar record which also resulted in significant flooding on Timber Creek. In addition, the storms analyzed for this study all had an areal extent large enough to cover the entire basin for the majority of the storm's duration. As such, this study examines the effects of within-storm rainfall variability on runoff generation. A summary of the storms used in this study and the radar locations where the data originated is provided in Table 1. A significant aspect of this study is the location of the radar with respect to the watershed being studied. It has often been noted that the performance of a weather radar tends to deteriorate at ranges far from the radar site [*Smith et al.*, 1996a]. Both of the radars used in this study are

located at a significant distance from the watershed (200 km for KTLX and 208 km for KFDR), leading to further difficulties in obtaining accurate estimation of precipitation. This issue highlights the importance of supplemental information from rain gauges to calibrate and adjust the radar.

Ten daily and hourly reporting rain gauges are located within 65 km of the outlet of the Timber Creek watershed; however, none of these is located within the watershed. With only these rain gauges a modeling study on Timber Creek would be very difficult. The precipitation measurements over the entire 100-km^2 basin would be dominated by the data collected from the closest gauge, poorly representing the rainfall heterogeneity which occurs over the basin. Nevertheless, the scattered rain-gauge measurements are very useful for calibration and adjustment of the radar-estimated precipitation. Of the ten gauges, four were "hourly reporting" and the other six were "daily reporting." The data from the four hourly reporting stations were obtained from the Western Regional Climate Center in Reno, Nevada. The gauges are believed to be of the Fisher-Porter type and report accumulated rainfall in tenths of an inch. The data for the daily reporting rain gauges were provided by the Southern Regional Climate Center in New Orleans, Louisiana.

Streamflow records for Timber Creek were obtained from the U.S. Geological Survey (USGS). These 15-min flow data were termed "provisional" by the USGS, indicating that the data had not been through all of the quality control procedures. Nevertheless, they were the best data available for the study. The streamflow data were used in calibrating several of the rainfall-runoff model parameters. In addition, a 50-m resolution digital evolution model (DEM) was created for the Timber Creek watershed from USGS 1:100,000 scale digital line maps. The topogrid function within the arc/info 7.0 Geographical Information System software was employed to convert these vector line maps to a raster DEM. With topogrid the user may specify the spatial resolution and various interpolation techniques to be used, as well as the filling of "sinks" to create a "hydrologically corrected" DEM (in a hydrologically corrected DEM, all of the water flows downhill toward the basin outlet by smoothing out local low regions). Finally, distributed soils data were obtained from the Natural Resource Conservation Service (previously the Soil Conservation Service). These data have a 250-m spatial resolution and contain, among other things, information on the USDA soil series classification. USDA soil surveys for Cooke County, Texas [*Putnam et al.*, 1979], and Grayson County, Texas [*Cochran*, 1980], were used to determine the various physical properties of interest for each soil type. Without a doubt, a great deal of uncertainty exists in both the soil types and especially the soil properties defined by the soils data set. The published soil types and properties were assumed to be true for the purposes of this study.

2.3. Rainfall-Runoff Model

The rainfall-runoff model for this study, hereafter called the Timber Creek Watershed (TCW) model, was required to be spatially distributed, event based, and able to simulate both infiltration-excess and saturation-excess runoff generation. A model structure which lends itself to use of radar-estimated precipitation is a spatially distributed grid-based discretization, such as that employed by the SIMPLE model [*Kouwen and Garland*, 1989; *Kouwen et al.*, 1993] and the European SHE model [*Abbott et al.*, 1986]. Such a structure was chosen for this study. An evapotranspiration component was not required, because the TCW model was to be run for short duration storm periods. A runoff routing component was also not required, because the primary emphasis was in assessing the effects of radar-estimated precipitation uncertainties on runoff volume generation. Both the infiltration-excess [*Horton*, 1933] and saturation-excess [*Dunne and Black*, 1970] runoff generation mechanisms were included in the TCW model, because of the suspicion that each responds differently to changes in precipitation input.

The TCW rainfall-runoff model developed for this study incorporated a *Green and Ampt* [1991] infiltration model to control the generation of infiltration-excess runoff and used the TOPMODEL [*Beven and Kirkby*, 1979] approach to control the generation of saturation-excess runoff. The Green-Ampt infiltration model is an approximate theory-based model which utilizes Darcy's law. It was originally developed to simulate infiltration under ponded conditions and was later modified by *Mein and Larson* [1973] to simulate infiltration during a rainfall event. Water is assumed to enter the soil as piston flow, producing a sharp wetting front between the wet and dry zones. Parameters needed for the Green-Ampt model include the effective hydraulic conductivity, the effective suction at the wetting front, the effective soil porosity, and the initial water content of the soil. Comprehensive tables and figures for estimating these parameters based on USDA soil texture data appear in the *Handbook of Hydrology* [*Rawls et al.*, 1993]. The Green-Ampt model does not explicitly account for accelerated infiltration rates due to macropores; however, such effects can be modeled by properly adjusting hydraulic conductivity [*Rawls et al.*, 1993]. The Green-Ampt model also does not account for lateral movement of soil water. This was not considered a great limitation for application to Timber Creek, because the gentle slopes of the watershed are not conducive to significant lateral fluxes of soil water, assuming small horizontal soil-moisture gradients. One of the primary reasons for choosing the Green-Ampt model to control infiltration-excess calculations was that parameters could be estimated from soil-texture data. This was especially suitable for parameterizing a spatially distributed infiltration model, for which calibration would be practically infeasible. The model parameters estimated from soil-texture data are likely a rough estimate of parameter values suitable for the 250 × 250 m areas which they were meant to represent. Nevertheless, the spatial heterogeneity of the infiltration process in Timber Creek is fully represented by the application of the Green-Ampt infiltration scheme within the TCW model, which was the objective of the infiltration-excess runoff component of the model.

TOPMODEL predicts the surface and subsurface hydrologic response of watersheds which experience surface runoff from variable saturated areas [see *Beven et al.*, 1995]. The TOPMODEL conceptualization is premised upon three basic assumptions: (1) The dynamics of the saturated zone can be approximated by successive steady state representations, (2) the hydraulic gradient of the saturated zone can be approximated by the local surface topographic slope, and (3) the distribution of downslope transmissivity with depth is an exponential function of storage deficit or depth to water table. These assumptions lead to relationships between the catchment soil storage deficit and the local water table level, where the main quantity used in the relationship is the topographic index $\ln(a/\tan b)$ introduced by *Beven and Kirkby* [1979], where a represents the upslope contributing area per unit

contour length and tan b is the local ground slope. In later modifications of the model the original topographic index was replaced by a combined topographic-soils index of the form $\ln(a/T_0 \tan b)$, where T_0 represents the transmissivity when the soil profile is fully saturated. This new formulation explicitly accounts for variability in local transmissivity in the index of hydrologic similarity. Furthermore, both the second and third assumptions listed above have recently been broadened to encompass a greater variety of hydrologic conditions observed in the field. Evidence from several studies has suggested that the hydraulic gradient in a watershed may be significantly influenced by the orientation of subsurface features, such as a shallow bedrock layer, requiring the use of a reference level to better approximate the water table surface [*Quinn et al.*, 1991]. In addition, the assumption of an exponential transmissivity function has been broadened to include parabolic and linear transmissivity functions, thought to better represent some watershed behavior [*Ambroise et al.*, 1996]. Because soils in the Timber Creek watershed are quite deep, surface topography was thought to be more significantly related to the local hydraulic gradient than the subsurface geologic structure. As such, the original TOPMODEL assumption was adopted. Regarding selection of the local transmissivity function, the original exponential function was chosen, as there was not any evidence that either the linear or parabolic functions would be more appropriate for Timber Creek.

The TCW model formulation allows for the infiltration-excess and saturation-excess runoff generation mechanisms to occur simultaneously or separately. The model was designed so that each runoff mechanism could be "turned on" or "turned off" so that the response of each mechanism to precipitation uncertainty could be evaluated independently. Although subsurface runoff contribution to streamflow was computed through the TOPMODEL portion of the TCW model, it was not included in the runoff volume analysis. The contribution of subsurface runoff to the total runoff volume was small compared to the contributions of surface runoff for the large events analyzed in this study. Thus the conclusions derived from this study will be most applicable for locations or storm events where surface runoff is the dominant contributor to streamflow.

3. Methods

3.1. Development of Radar-Estimated Precipitation Data

One of the objectives of this study was to examine the effects of the uncertainty in the transformation of radar reflectivity to rainfall on predicted runoff generation from a watershed. A portion of this uncertainty was assumed to be due to the variability in the parameter values of the power law model used to transform reflectivity into rainfall rate, shown by (1) as

$$Z = aR^b \tag{1}$$

where

Z radar reflectivity [dBZ];
R rainfall rate $[L/T]$;
a radar coefficient;
b radar exponent.

It is well documented that values of the parameters a and b in the radar equation are not constant in time or in space [*Martner*, 1977; *Smith et al.*, 1996b], and several authors have suggested different values for specific situations [*Battan*, 1973; *Collier*, 1989]. The parameters a and b depend theoretically on the hydrometeor drop-size distribution within a given sample volume of the atmosphere, and it is intuitive that this distribution may vary considerably from storm to storm and even across different sections of the same storm. Although certainly not the only factor which contributes uncertainty to the transformation of reflectivity to rainfall rate (others include radar hardware calibration, reflectivity field contamination by hail and bright band effects, and anomalous propagation [*Smith et al.*, 1996a]), it is a significant one.

To consider the effects of this source of uncertainty in radar-estimated precipitation on runoff predictions, three scenarios for determining the values of a and b were considered. In the first scenario the values of the parameters were set at the "default" parameters suggested by the NEXRAD algorithm developers. In the second scenario the parameters were calibrated for a small region of the radar umbrella corresponding to the area immediately surrounding the study site. In this scenario, all of the storms being studied were used together to find one optimal set of parameter values for all the storms. In the third scenario the parameters a and b were calibrated for each storm event separately, consistent with the notion that these parameters vary from storm to storm.

The calibration of the parameters in the radar equation was performed using the Shuffled Complex Evolution (SCE-UA) global search algorithm [*Duan et al.*, 1992]. This method has proven to be very efficient in locating the optimal set of parameter values and was more than sufficient for calibration of the simple two-parameter radar equation. The objective function employed in the calibration procedures is described by (2):

$$\text{Min } F = \sum_{j=1}^{m} \sum_{i=1}^{n} |G_i^j - R_i^j| \tag{2}$$

where

G gauge storm total precipitation (L);
R radar storm total precipitation (L);
m number of storms;
j storm number;
n number of gauges for storm j;
i gauge number for storm j.

This objective function, which minimizes the absolute value of the radar-gauge difference, was chosen so that roughly equal emphasis would be placed on the small storms as on the large storms and, similarly, on the gauges with high precipitation and low precipitation.

A procedure which is sometimes used to improve the estimation of rainfall from radar is to perform additional bias adjustments with rain-gauge data. In the NEXRAD precipitation-processing algorithm a Kalman filter is employed, incorporating hourly gauge precipitation in real time to determine a mean field bias in the radar estimates of precipitation [*Seo et al.*, 1995]. Other simpler methods have been suggested by *Collinge* [1991] which compute a bias correction factor simply on the basis of the ratio of the precipitation measured by the rain gauges to the precipitation estimated by the radar. This type of bias correction was used in this study and is given by (3) as

$$\mathrm{CF}_i = \frac{\sum_{j=1}^{n} G_i^j}{\sum_{j=1}^{n} R_i^j} \tag{3}$$

where

CF bias correction factor;
G gauge storm total precipitation (L);
R radar storm total precipitation (L);
n number of gauge/radar pairs;
i storm number;
j gauge number.

The bias correction factor is computed on a storm-by-storm basis using all or some of the ten gauges surrounding Timber Creek. The computed bias is specific only to the location surrounding Timber Creek and would not apply to other regions of the radar umbrella. Once the correction factor is calculated, a new value is obtained for each radar pixel according to (4) as

$$\mathrm{RA} = R \times \mathrm{CF}_i \tag{4}$$

where

RA adjusted radar precipitation [L/T];
R original radar precipitation [L/T];
CF_i bias correction factor for storm i.

The bias correction factor was either applied or not applied, resulting in two alternatives in the precipitation processing procedure employed.

Permutations of the three scenarios for determining the values of the radar equation parameters a and b and the two scenarios for incorporating a bias correction factor result in six different methods for developing radar-estimated precipitation data for each storm. These six methods represent the range in precipitation data obtainable by different precipitation processing techniques which may be employed by independent users of NEXRAD Level II base reflectivity data. For each method the same preprocessed reflectivity images were used. Preprocessing of the reflectivity data was performed using a simplified version of that employed by the NEXRAD algorithm [see *Winchell et al.*, 1997].

The performances of each of the six methods employed were evaluated statistically by comparing the resulting rain gauge–radar pixel pairs. While some of the techniques produced better matches between the gauges and radar, the results of these comparisons will not be discussed at this time. Instead, we are concerned here with the fact that the techniques represent a range of possible methods for constructing precipitation information from NEXRAD Level II data and may result in a range of runoff predictions. For a complete discussion of the performance of the different precipitation processing techniques, refer to *Winchell et al.* [1997].

3.2. Aggregation of Precipitation Data

The base-level precipitation data sets generated according to each of the six techniques were constructed using the 1 × 1 km, 6-min reflectivity data. A more common spatial resolution for quantitative radar-estimated precipitation, such as the 4 × 4 km, 1-hour NEXRAD product, is considered to be sufficient for modeling larger main stem river basins, yet it may not contain enough detail to properly reflect small-scale rainfall features important in the hydrologic response of smaller basins susceptible to flash flooding. A temporal resolution of the order of 6 min is able to depict transient rainfall characteristics which define small-scale runoff production in most situations, as suggested by *Krajewski et al.* [1991] and *Michaud and Sorooshian* [1994]. Trouble arises when variable intensity rainfall events are assumed to have a constant intensity for longer periods of time. While assuming that a constant rainfall intensity duration of 1 hour may be suitable for large basin hydrologic prediction, modeling basins of the order of 200 km^2 or smaller may require more accurate capturing of the short-duration rainfall dynamics, especially for convective type events. The question of how much aggregation of this "high"-resolution rainfall data can occur before significant effects on runoff prediction occur is a primary issue explored in this paper.

The bulk of this study consists of a sensitivity analysis performed to investigate the effects of spatial and temporal aggregation of the radar-estimated precipitation data on runoff generation. Spatial resolutions of 2 km, 4 km, 8 km, and 16 km were generated from the original 1-km data. For each spatial resolution, 24-min, 42-min, and 60-min temporal resolution precipitation estimates were generated from the original 6-min resolution data. This resulted in 20 different precipitation data sets for each of the seven storms studied. These different precipitation data sets were used as input to the TCW rainfall-runoff model to assess sensitivity of both the saturation-excess response and the infiltration-excess response.

3.3. Rainfall-Runoff Model Calibration

Calibration of a limited number of rainfall-runoff model parameters was necessary for proper implementation of the TCW model. Although this study is not specifically concerned with assessing the performance of a rainfall-runoff model or testing a calibration procedure, it is important that the hydrologic model produce realistic simulations if proper value is to be given to the results of later experiments. Because the emphasis of this study was on examining the sensitivity of surface-runoff generation to precipitation uncertainty, the calibration procedure was designed to minimize the difference between observed and simulated surface-runoff volume. This required separating surface runoff and base flow from the observed streamflow records. The base flow separation technique used for this study was centered on the development of a master base flow recession curve for the watershed, used to determine the time at which surface runoff ends. For a description of this technique, refer to *Chow et al.* [1988].

The Shuffled Complex Evolution automatic optimization routine [*Duan et al.*, 1992] was used to identify the parameters for the TCW model. The only parameters which required calibration were the TOPMODEL transmissivity scaling parameter m and the initial soil-moisture conditions θ_i for each of the seven storms studied. The remaining parameters were estimated from published soil data. Although the initial soil-moisture conditions technically are not model parameters, they were calibrated in conjunction with the TOPMODEL m parameter. The calibration was arranged such that data from five of the seven storms were used to identify m and the five θ_i values. Afterward, the θ_i values for the remaining two storm events were determined using the m value obtained from the five-storm calibration.

The objective function used in the optimization program was the absolute difference between observed and simulated sur-

Table 2. Calibration Results

Storm Date	Observed Surface Runoff, mm	Simulated Surface Runoff, mm	m, cm	θ_i, cm/cm	10-Day Antecedent Precipitation
Oct. 28, 1991	31.9	31.7	0.234	0.944	4.17
Oct. 31, 1991	35.4	35.3	0.234	0.999	5.60
Sept. 10, 1992	17.5	18.1	0.234	0.775	3.05
Feb. 24, 1992	21.2	20.8	0.234	0.941	1.86
May 9, 1993	61.6	61.7	0.234	0.774	0.41
May 12, 1994	25.7	25.2	0.234	0.963	1.54
April 10, 1995	9.0	9.0	0.234	0.956	1.50

Initial soil moisture θ_i is expressed as a fraction of local field capacity.

face runoff volume. This objective function formulation is expressed in (5) as

$$\text{Min } F = \sum_{i=1}^{n} |Qs'_{obs} - Qs'_{sim}| \quad (5)$$

where

F objective function value [L];
Qs_{obs} observed surface-runoff volume [L];
Qs_{sim} simulated surface-runoff volume [L];
i storm number;
n number of storms in calibration.

The simulated surface runoff for the calibration was generated with the 1 × 1 km, 6-min resolution precipitation input.

The results of the TCW model calibration are shown in Table 2. The observed and simulated runoff volume, the TOPMODEL m parameter value, and the θ_i values are shown for each storm. The observed and simulated surface-runoff volumes are nearly identical. This was achievable through the calibration of the initial soil-moisture conditions. The θ_i values represent the initial soil moisture as a fraction of the local field capacity. The local field capacity is dependent on soil type and varies through the watershed. This allows for the volumetric soil-moisture content to vary as a function of local field capacity. While the θ_i values are all relatively high, they are not unreasonable considering the time of year and the 10-day antecedent precipitation, also shown in Table 2 (recall that because these were some of the largest runoff events during the period of study, wet conditions should be expected). While the calibration of the TCW model parameters was relatively simple, it verified that the model was capable of producing surface-runoff amounts comparable to those observed.

4. Results

4.1. Sensitivity of Runoff Generation to Reflectivity-Rainfall Transformation Uncertainty

The range in possible precipitation information obtained from the original reflectivity data was represented by the six different techniques for calibrating and adjusting the radar data with rain gauges. The calibration and bias adjustment combination defining methods 1–6 are given in Table 3. Each of these sets of data were used as input to the TCW rainfall-runoff model to see how runoff generation is affected by the uncertainty inherent in the transformation of reflectivity to rainfall. The quantity being compared for each of the cases studied is the cumulative surface runoff generated during the storm period. Where indicated, the cumulative runoff shown may only be the saturation-excess portion or the infiltration-excess portion. The fractions of "true" runoff produced from each of the six different precipitation data sets for the seven storms studied are shown in Figure 1. The fraction of true runoff is plotted on the y axis, and the calibration/adjustment method is plotted on the x axis. Each of the lines on the graph represents a different storm event. The true runoff is assumed to be that which occurred from using the precipitation generated using method 6, because method 6 was found to produce the best fit between the rain gauges and the radar [*Winchell et al.*, 1997].

Several important conclusions are made from Figure 1. First, the volume of simulated surface runoff is strongly dependent upon the method used to construct the precipitation input. This is shown by how much the fraction of true runoff varies from method 1 to method 6 for an individual storm. Second, Figure 1 shows that simulated runoff from some storms is more sensitive to the precipitation calibration/adjustment method than other storms. For example, the fraction of true runoff generated for one storm varied from 0 to 1.0, while another

Table 3. Radar Calibration Methods

Calibration Method	Radar Equation Parameters	Bias Correction Factor
1	default	not applied
2	storm independent	not applied
3	storm dependent	not applied
4	default	applied
5	storm independent	applied
6	storm dependent	applied

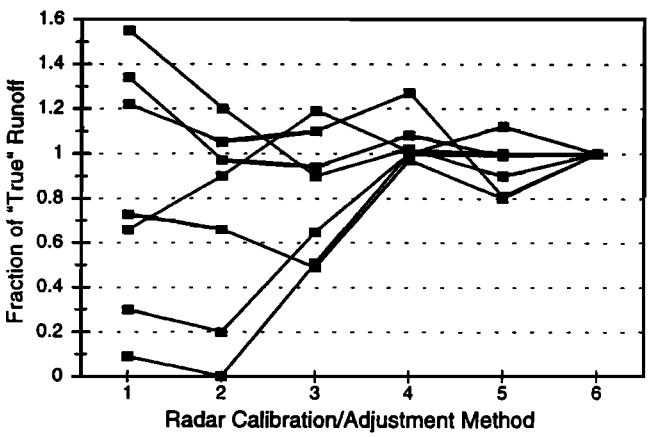

Figure 1. Runoff sensitivity to radar calibration/adjustment method; "true" runoff represents runoff generated from method 6 precipitation input. Each line represents a different storm.

varied only from 0.94 to 1.34. Finally, the value in calibrating parameters in the Z-R relationship, as well as incorporating a local bias adjustment to the precipitation estimation procedure, is well supported. It is fair to say that radar calibration/adjustment methods 4–6, which incorporated a bias correction factor, resulted in better runoff simulations than methods 1–3, which did not incorporate a bias correction factor. Furthermore, the methods which incorporated storm-dependent Z-R parameter calibration, methods 3 and 6, produced better runoff simulations than methods 1–2 and 4–5, respectively. This analysis emphasizes the significant errors that can result in runoff predictions as a result of uncertainty in the precipitation input. It also advises using methods for obtaining precipitation data from radar reflectivity which attempt to reduce the uncertainty in the reflectivity to rainfall transformation.

Using the same six sets of precipitation input, the cumulative runoff volume was calculated separately for the infiltration-excess response and the saturation-excess response. Along with investigating whether these two types of runoff responded differently to varying precipitation input, it was desired to determine how the resulting errors in runoff compared with the errors in rainfall. The assumption will be made that the "true" rainfall is that produced according to method 6 and that the true runoff is that resulting from the true rainfall. A plot of the rainfall error versus the saturation-excess and infiltration-excess runoff error for all six precipitation data sets and all seven storms studied are presented in Figure 2. The 1:1 line represents equally sized errors for rainfall and runoff. For saturation-excess runoff (Figure 2a) the magnitude of the runoff errors is the same or slightly larger than the size of the corresponding rainfall errors. While this rainfall error is quite significant at times (up to −80%), we do not see dramatically larger errors in runoff. Furthermore, the relationship between rainfall errors and runoff errors is generally linear. In the infiltration-excess case (Figure 2b), much different behavior is observed. Here very small rainfall errors (10%) can result in runoff errors up to 170%, illustrating the extreme sensitivity of infiltration-excess runoff generation to the rainfall input. Furthermore, the relationship appears to be highly nonlinear as opposed to the relatively linear behavior of the saturation-excess runoff.

The difference in the behavior between the saturation-excess and infiltration-excess runoff generation is expected. Because saturation-excess runoff occurs only when the local soil profile is saturated, the infiltration rate of that soil region is essentially zero. For a unit increase in rain falling on that

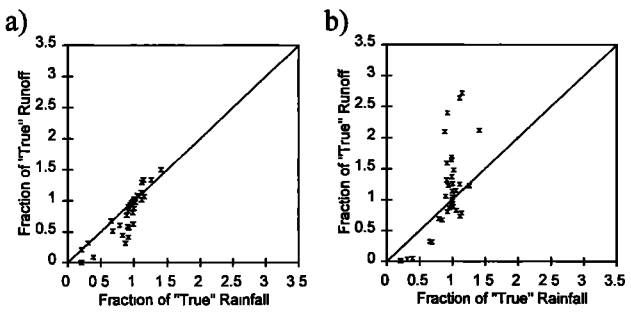

Figure 2. Rainfall error versus runoff error resulting from the six different sets of precipitation input: (a) saturation-excess and (b) infiltration-excess runoff; all storms are included.

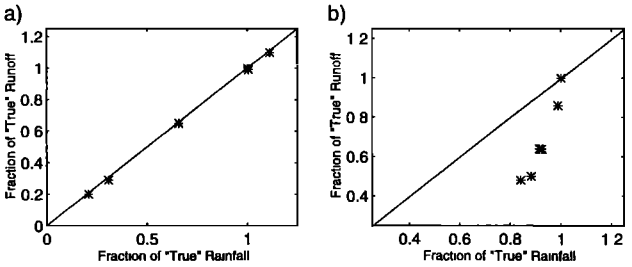

Figure 3. Rainfall errors versus saturated-excess runoff error for (a) "wet" (October 31, 1991) antecedent conditions and (b) "dry" (September 10, 1992) antecedent conditions.

saturated area a unit increase in runoff generation will result. Thus a 20% increase in rainfall will result in a 20% increase in runoff from a saturated area. Of course, the dynamics of the expanding saturated areas add some complication to this; however, this serves primarily to change the slope of the linear relationship between rainfall errors and runoff errors. This can be seen by examining Figure 3, which plots the rainfall error versus runoff error for two individual storms. One storm, from September 10, 1992, occurred under very dry antecedent conditions, while the other storm, from October 31, 1991, occurred under very wet antecedent conditions. Both plots indicate a nearly linear relationship; however, the slope for the "wet" watershed case is ~1, while the slope for the "dry" watershed case is significantly greater than 1. In the wet case a unit change in runoff results from a unit change in rainfall because a large percentage of the basin is saturated. In the dry case, small changes in rainfall result in larger changes in runoff because some of the areas of the watershed do not become saturated when the rainfall changes. The behavior seen here agrees with *Numec* [1985] that errors in precipitation input have a more serious effect on runoff modeling when the catchment is dry. The dramatic response of the infiltration-excess runoff to rainfall variations is a direct result of the highly nonlinear nature of the infiltration process. Although the total rainfall volume may experience only slight changes, the rainfall intensity structure may have been sufficiently altered to cause radically different interactions with the local infiltration rate of the soil.

This analysis suggests that when modeling the infiltration-excess type of runoff, caution should be exercised when the quality of the precipitation data is in question. If saturation-excess is the runoff-generation mechanism being modeled, then the size of the simulated runoff errors may only be as large as the errors in the rainfall. Of course, this might change depending on the basin conditions, with a drier basin being more susceptible to larger runoff errors. Section 4.2 will examine how errors in the rainfall due to changing the resolution of the data affect runoff predictions.

4.2. Sensitivity of Runoff Generation to Precipitation Aggregation

This section focuses on the sensitivity of surface-runoff generation to the spatial and temporal resolution of radar-estimated precipitation. This section also considers how aggregation in time and space of high-resolution radar-estimated precipitation data affects both the infiltration-excess and the saturation-excess modes of surface-runoff generation. This is an important issue, because many current hydrologic models utilize precipitation input that has undergone some degree of spatial and/or temporal aggregation. The spatial resolutions of

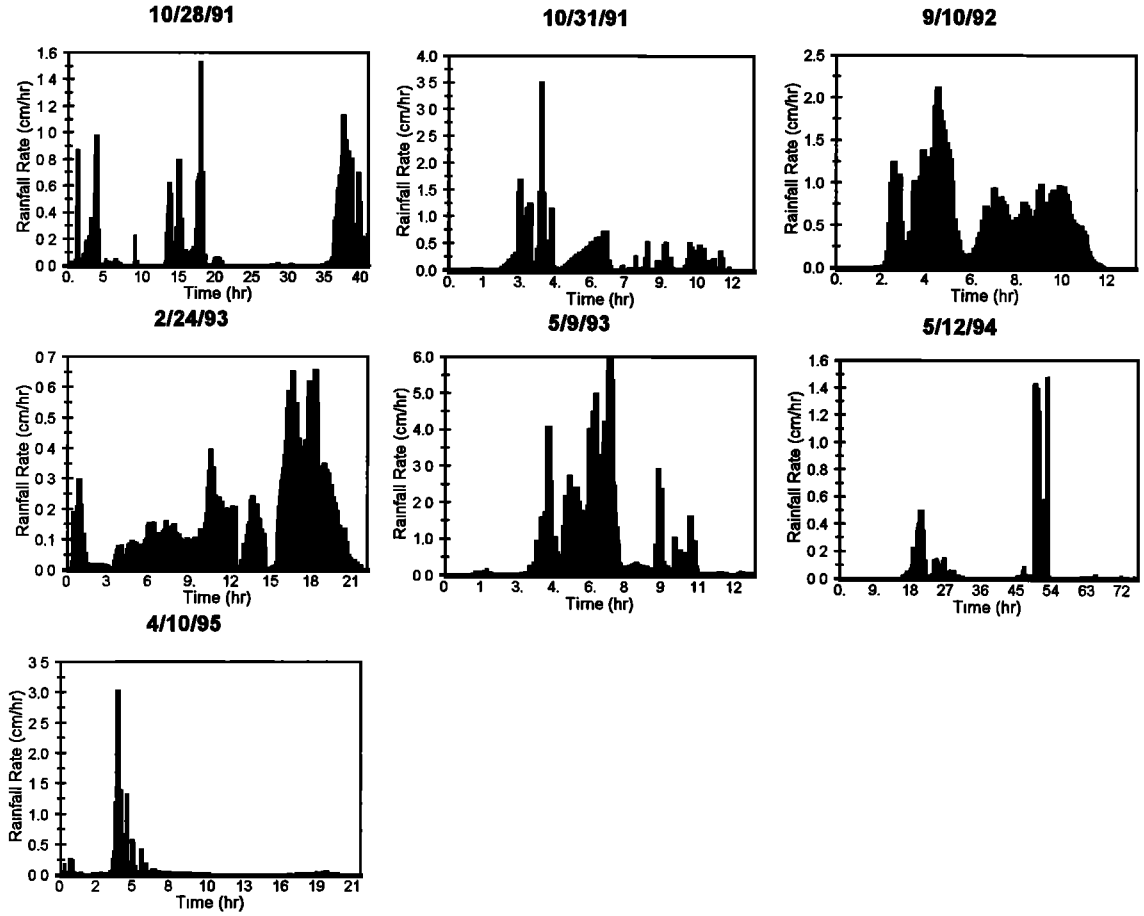

Figure 4. Mean basin-average hyetographs for the storm events studied.

the precipitation data that will be considered here include (1) 1 × 1 km, (2) 2 × 2 km, (3) 4 × 4 km, (4) 8 × 8 km, and (5) 16 × 16 km. The temporal resolutions considered include (1) 6 min, (2) 24 min, (3) 42 min, and (4) 60 min. Basin-average hyetographs for each of the seven storms studied are shown in Figure 4. These hyetographs are based on the original 6-min data, before any temporal aggregation. The first set of sensitivity analyses considered will not force basin precipitation volume to be conserved across aggregation levels. A second set of sensitivity analyses will keep basin precipitation volumes preserved in an effort to remove the effects of mapping errors for comparison purposes.

The effect of precipitation aggregation on saturation-excess runoff generation for four different storms is shown in Figure 5. Each of the subplots represents a different storm. The x axis represents the temporal resolution of the precipitation input, the y axis represents the fraction of true runoff (runoff from 1-km 6-min precipitation input) generated from a given precipitation resolution, and each line on the plot refers to the spatial resolution of the input. As seen in Figure 5, there is essentially no sensitivity of the runoff generation to the temporal resolution of the input. This indicates that saturation-excess runoff is not dependent on the intensity structure of the rainfall. However, when the spatial aggregation of the input is changed, the runoff volumes do change. For the case of September 10, 1992, there is a 50% increase in the runoff volume given the 16-km resolution input. For this particular storm a trend for the coarser resolutions to produce more runoff is observed. For the storm of October 31, 1991, the trend is for coarser resolutions to produce less runoff. The May 9, 1993, storm shows peculiar behavior in that the 16-km resolution produces the most runoff and the 8-km resolution produces the least. The April 10, 1995, storm shows some inconsistencies as well. A feature of interest from Figure 5 is that among the storms studied, there is no consistent trend for more or less runoff to be produced as the level of precipitation aggregation is increased. Furthermore, the magnitudes of the changes generally are not very large, being of the order of 10–15% for most cases.

The effect of precipitation aggregation on infiltration-excess runoff is shown in Figure 6. Once again, each of the subplots represents a different storm. Much different behavior is observed than for the saturation-excess runoff case. First, there is considerable sensitivity to the temporal resolution on the rainfall input. The 1-hour, 1-km precipitation input results in 58% less runoff than the 6-min 1-km precipitation input for the October 31, 1991, storm. The general trend for all of the storms is for increasing temporal aggregation of the precipitation to result in decreasing amounts of runoff. As for the effects of spatial aggregation of the precipitation on runoff generation, there is somewhat of a trend for the coarser resolutions to produce less runoff; however, this is not entirely consistent. The October 31, 1991, and the May 9, 1993, storms are mostly consistent with this behavior; however, the April 10, 1995, storm shows numerous occasions where this trend is violated. For example, the 8-km and 16-km resolution inputs

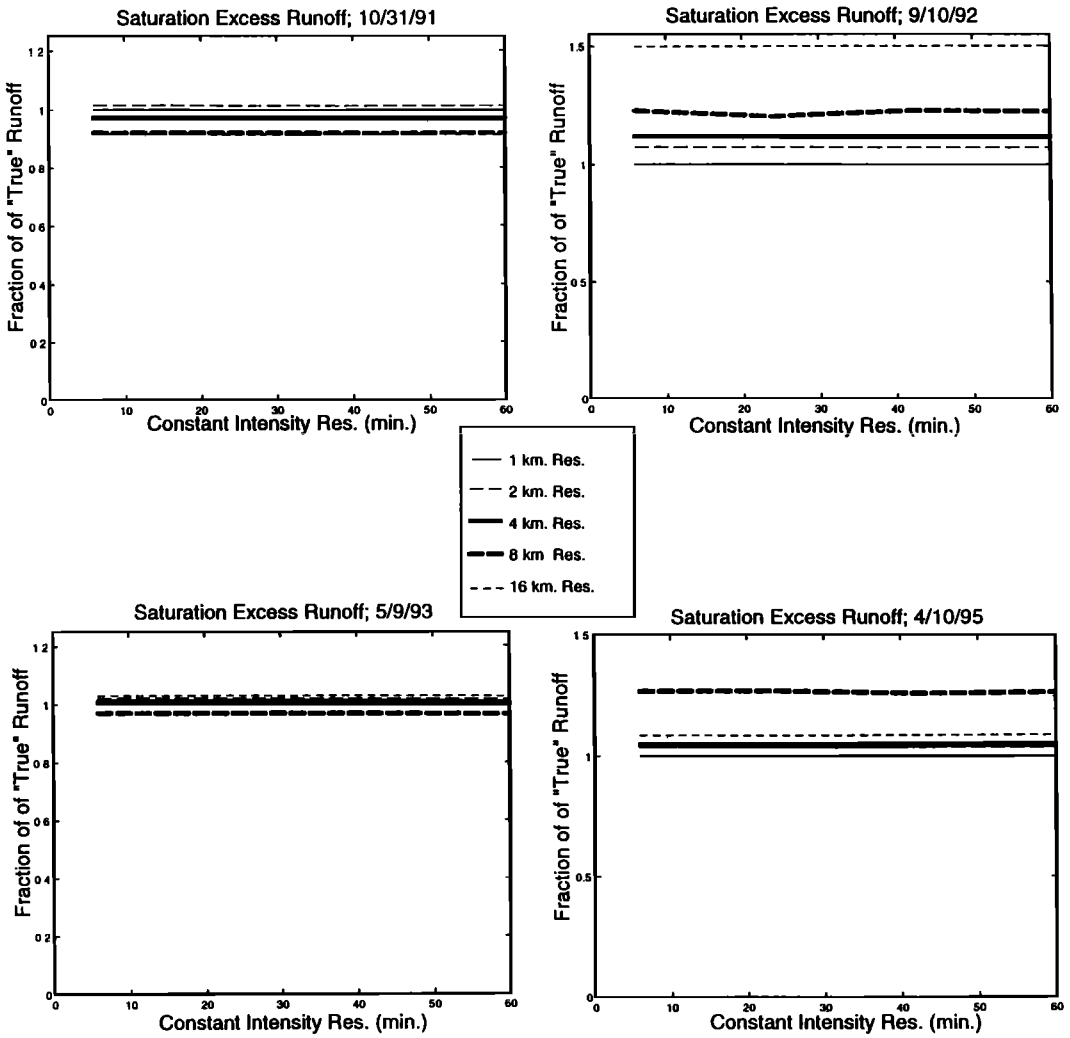

Figure 5. Saturation-excess runoff sensitivity to temporal and spatial resolution of precipitation input.

for the longer temporal resolutions produce significantly more runoff than the higher spatial resolutions. For the September 10, 1992, storm the trend is strictly for the coarser resolutions to produce more runoff. Intuitively, it is expected that coarser spatial resolution precipitation should result in less infiltration-excess runoff, because the localized high-intensity rainfall regions are being smoothed out. It is these high-intensity rainfall regions that are most important in generating infiltration-excess runoff.

The inconsistencies in the behavior of the infiltration-excess runoff response to spatial aggregation of the precipitation, and all of the sensitivity of the saturation-excess response, are due to changes in total rainfall volume falling within the watershed. This change in rainfall volume falling within the watershed can be considered a mapping error and occurs as follows. Typical spatially varying rainfall patterns consist of regions of heavier or lighter precipitation outside the immediate boundaries of a watershed. For example, an individual convective cell may have moved just to the outside of the watershed boundary, dropping a swath of heavy precipitation. Inside the watershed boundary the mean precipitation depth may be much less than what was dropped by the convective cell. If an aggregation of pixel-based precipitation is performed over the region surrounding this watershed and a new mean precipitation depth for the watershed is calculated, then the resulting value will be larger than the original mean watershed precipitation depth because of the influence of the convective cell outside the true watershed boundary. A hypothetical example of this is shown in Figure 7. In this example the original rainfall data are aggregated from a 1×1 cell grid to a 3×3 cell grid. In doing so, the apparent total volume of precipitation falling within the watershed boundary is reduced because of the areas of lighter precipitation falling outside of the watershed boundary. Thus spatial aggregation of precipitation can serve to either increase or decrease the volume of rain falling within a watershed. It is this process of "smoothing precipitation volume" which has caused the irregular sensitivity of the saturation-excess runoff to spatial resolution of the rainfall and the inconsistent sensitivity of the infiltration-excess response. This is essentially the same process observed and described by *Ogden and Julien* [1994].

The information in Table 4 supports the direct relationship found between rainfall volume and saturation-excess runoff volume for the different spatial resolutions of precipitation tested. For each storm event a "rank" is given to the spatial resolution which produced the greatest through least amount of rainfall volume and runoff volume. Examining the table reveals that the rainfall rank and the runoff rank match for every occasion. To determine if this "smoothing of precipita-

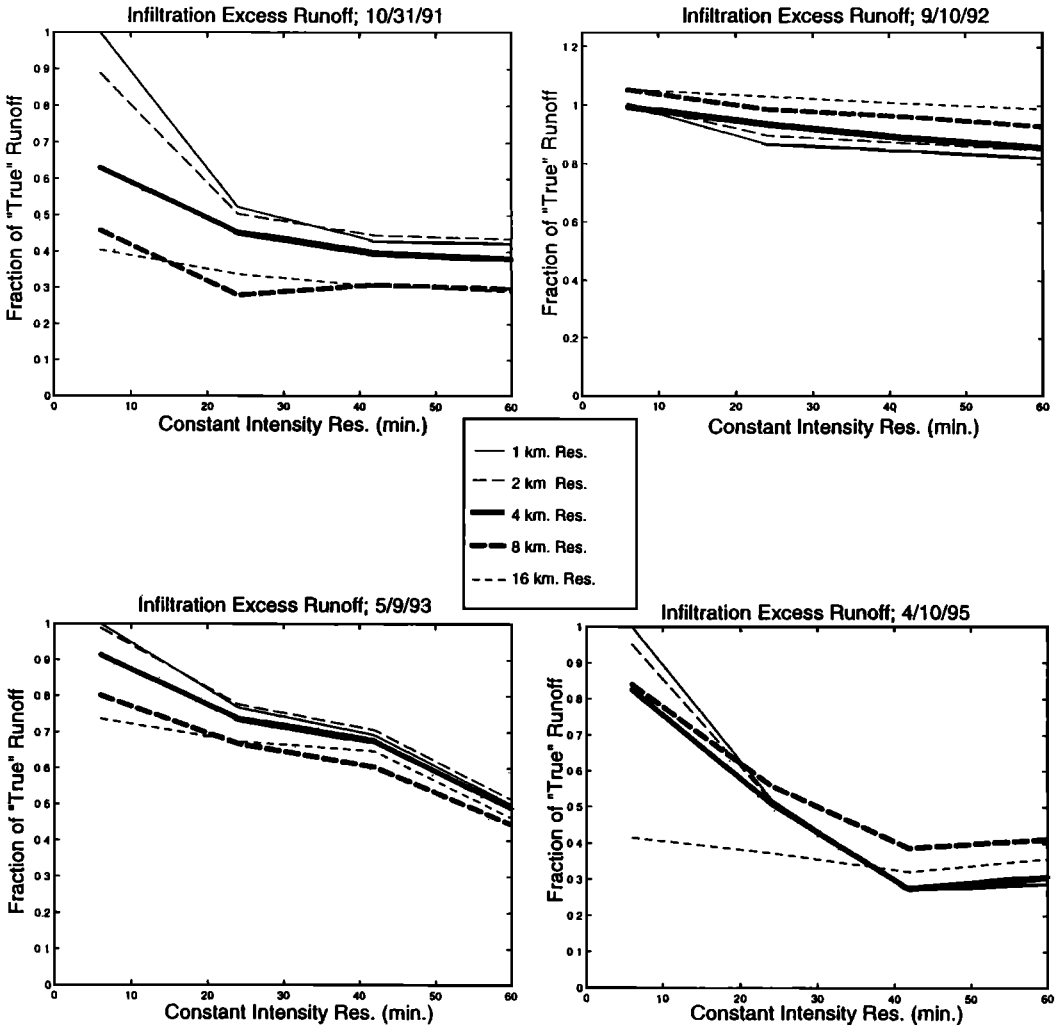

Figure 6. Infiltration-excess runoff sensitivity to temporal and spatial resolution of precipitation input.

tion volume" was exclusively responsible for the sensitivity of the saturation-excess runoff volume to spatial aggregation of the rainfall, the total rainfall produced by each spatial resolution was normalized to be that which was produced by the 1-km resolution data. In this case, the spatial aggregation is serving only to smooth the variability in rainfall intensity patterns throughout the basin, while the total rainfall volume remains constant. The sensitivity of saturation-excess runoff to aggregation of the precipitation input with "normalized" precipitation volume is displayed in Figure 8. For each of the storms shown, there is essentially no sensitivity to precipitation aggregation of any kind. For the September 10, 1992, storm the effect of precipitation aggregation on the runoff is much smaller than before. This slight sensitivity may be due to the method by which the precipitation was normalized, which simply applied the same adjustment at each time step and did not take into account the time-variant nature of the rainfall volume errors. These results indicate that if the change in precipitation volume falling in a basin due to spatial aggregation is properly accounted for, the temporal and spatial resolution of a radar-derived precipitation input will be inconsequential in the generation of saturation-excess runoff.

The effect of spatial and temporal aggregation on infiltration-excess runoff generation with normalized precipitation volume for the same storms previously shown are given in Figure 9. Comparing Figure 9 with Figure 6, significant differences are observed in the response of the runoff generation to changes in the spatial resolution. For the May 9, 1993, storm the trend for coarser spatial resolution to produce less runoff is not violated. The October 31, 1991, storm behavior becomes more consistent for the 1-km and 2-km resolutions at longer temporal resolutions, and the April 10, 1995, storm becomes much better behaved as well. The September 10, 1992, storm changes the most dramatically, with the expected behavior occurring for the normalized precipitation volume case. Obviously, the smoothing of precipitation volume plays a significant role in infiltration-excess runoff generation. When these effects are removed, a clear trend for runoff volumes to decrease with increasing temporal and spatial aggregation is observed.

The results of the discussion above support the findings of both *Obled et al.* [1994] and *Krajewski et al.* [1991]. Recall that Obled et al. found that runoff generation was sensitive to spatial information in the precipitation but insensitive to temporal information by using TOPMODEL to simulate saturation-excess runoff. Krajewski et al. found runoff generation to be sensitive to both the spatial and temporal information in the precipitation by simulating infiltration-excess runoff. This study has verified that the differences in the conclusions from

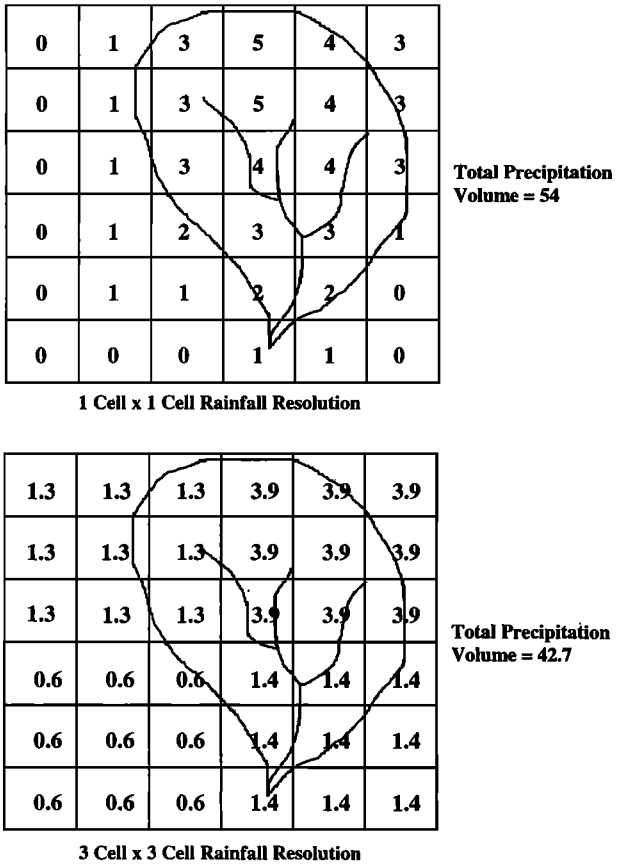

Figure 7. Reduction in watershed precipitation due to smoothing of precipitation volumes from spatial aggregation; hypothetical case.

these two earlier studies are a result of the different runoff models employed. An issue which was not significantly addressed in previous work is the variation in the sensitivity of runoff generation to precipitation resolution from storm to storm. The magnitude of the sensitivity of the runoff generation to various levels of rainfall aggregation differs among the four storms shown (Figure 9). The simulated runoff from the September 10, 1992, storm is much less sensitive to the precipitation resolution than the other storms. A storm-dependent parameter may exist which dictates how significantly predicted runoff from a given storm will be affected by aggregation of the precipitation input. These issues warrant additional investigation and are explored in section 4.3.

4.3. Estimation of Infiltration-Excess Runoff Reduction Due to Precipitation Aggregation

The storm characteristics thought to be most related to the effects of precipitation aggregation on runoff generation are those related to the spatial variability of the rainfall over the watershed area. The rainfall characteristics of a storm can be represented in many possible ways, such as the total rainfall depth, the average rainfall intensity, or the maximum rainfall intensity. The rainfall characteristic thought to be most relevant in producing infiltration-excess runoff is the maximum precipitation intensity, because it is the high-intensity periods that determine when and where runoff occurs. The spatial variability of these characteristics also can be represented in many ways, ranging from simple methods, such as determining the variance or standard deviation, to more complex methods, such as variogram analysis. Because the intent of this exercise was to develop a simple means for accommodating for errors in runoff simulation due to precipitation aggregation, the use of simple spatial variance of rainfall characteristics was chosen. Therefore the expectation was that the spatial variability of the highest rainfall intensity periods would be related to how sensitive the runoff generation would be to smoothing the rainfall input in time and space.

The specific statistic used to represent this was the spatial standard deviation of the maximum precipitation intensity (hereafter referred to as σ_{MaxInt}). Mathematically, it is calculated according to (6) as

$$\sigma_{\text{MaxInt}} = \sqrt{\frac{1}{1-n}\sum_{i=1}^{n}(\bar{I}_{\max} - I^{i}_{\max})^2} \tag{6}$$

where

σ_{MaxInt} spatial standard deviation of maximum intensity $[L/T]$;

n number of 1 × 1 km radar pixels over watershed area;

$\bar{I}_{\max}$ mean of maximum precipitation intensity for all pixels $[L/T]$;

Table 4. Comparison Between Ranking of Precipitation Volume in Watershed and Saturation-Excess Runoff Generation

Event	1-km Rank	2-km Rank	4-km Rank	8-km Rank	16-km Rank
Oct. 28, 1991 Precipitation	2	1	3	4	5
Oct. 28, 1991 Runoff	2	1	3	4	5
Oct. 31, 1991 Precipitation	2	1	3	4	5
Oct. 31, 1991 Runoff	2	1	3	4	5
Sept. 10, 1992 Precipitation	5	4	3	2	1
Sept. 10, 1992 Runoff	5	4	3	2	1
Feb. 24, 1993 Precipitation	5	3	4	2	1
Feb. 24, 1993 Runoff	5	3	4	2	1
May 9, 1993 Precipitation	4	2	3	5	1
May 9, 1993 Runoff	4	2	3	5	1
May 12, 1994 Precipitation	4	1	3	2	5
May 12, 1994 Runoff	4	1	3	2	5
April 10, 1995 Precipitation	5	4	3	1	2
April 10, 1995 Runoff	5	4	3	1	2

Here 1 represents "greatest" and 5 represents "least."

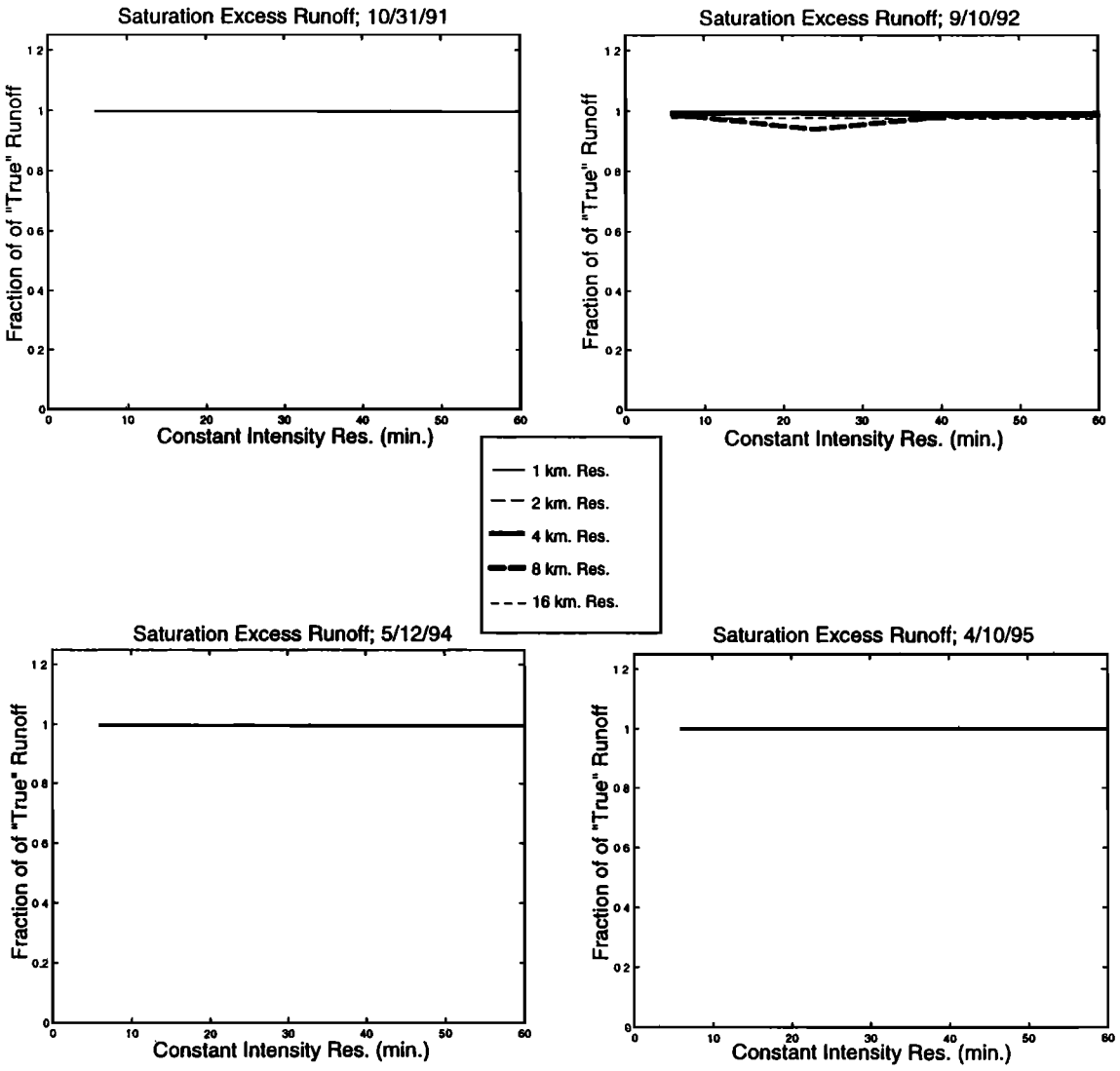

Figure 8. Saturation-excess runoff sensitivity to temporal and spatial resolution of normalized precipitation input.

$I^i_{\max}$ maximum precipitation intensity for pixel i $[L/T]$.

The maximum precipitation intensity at each pixel was determined by checking the rainfall intensity at each 6-min time step to see if it was greater than the previous maximum intensity.

The σ_{MaxInt} is plotted against the fraction of true runoff generated from different temporal (Figure 10) and spatial (Figure 11) resolutions. The σ_{MaxInt} exhibits a strong correlation with the reduction of runoff. For the cases of temporal aggregation, there is an approximate linear relationship between the σ_{MaxInt} and the fraction of true runoff produced at each of the different levels of aggregation. Recall that the true runoff refers to that which was produced by using the highest resolution precipitation data as input. In addition, the increase in runoff reductions with increased temporal aggregation is also apparent, shown by the negative slope of the least squares line increasing as the level of temporal aggregation moves from 24 to 60 min. Similarly, an approximate linear relationship between the σ_{MaxInt} and the reduction of runoff exists for the different cases of spatial aggregation (Figure 11). Again, the increasing negative slope of the least squares line as the spatial aggregation goes from 2 to 16 km indicates how the increasing spatial aggregation results in increasing runoff reductions. The lack of scatter of the data around the least squares line is remarkable. This suggests the possibility of determining runoff corrections on the basis of the linear relationships found in these plots.

Regression equations were developed to relate the fraction of true runoff generated by a given level of precipitation aggregation to the σ_{MaxInt} determined from the finest 1-km × 6-min precipitation resolution. A different equation was developed for each level of spatial and temporal aggregation. Each equation estimates the correction in simulated infiltration-excess runoff generation required, given the resolution of precipitation input and a knowledge of the variability in the storms' maximum precipitation intensity. These equations and their associated r^2 and correlation statistics are provided in Tables 5 and 6. The information shown in Table 5 indicates good fits between simulated and actual runoff reductions due to temporal aggregation. The performance of the regression equations is better for the coarser 42- and 60-min resolutions, suggesting that this relationship may be most effective at predicting runoff corrections due to significant aggregation. For the cases of the different spatial resolutions (Table 6) the

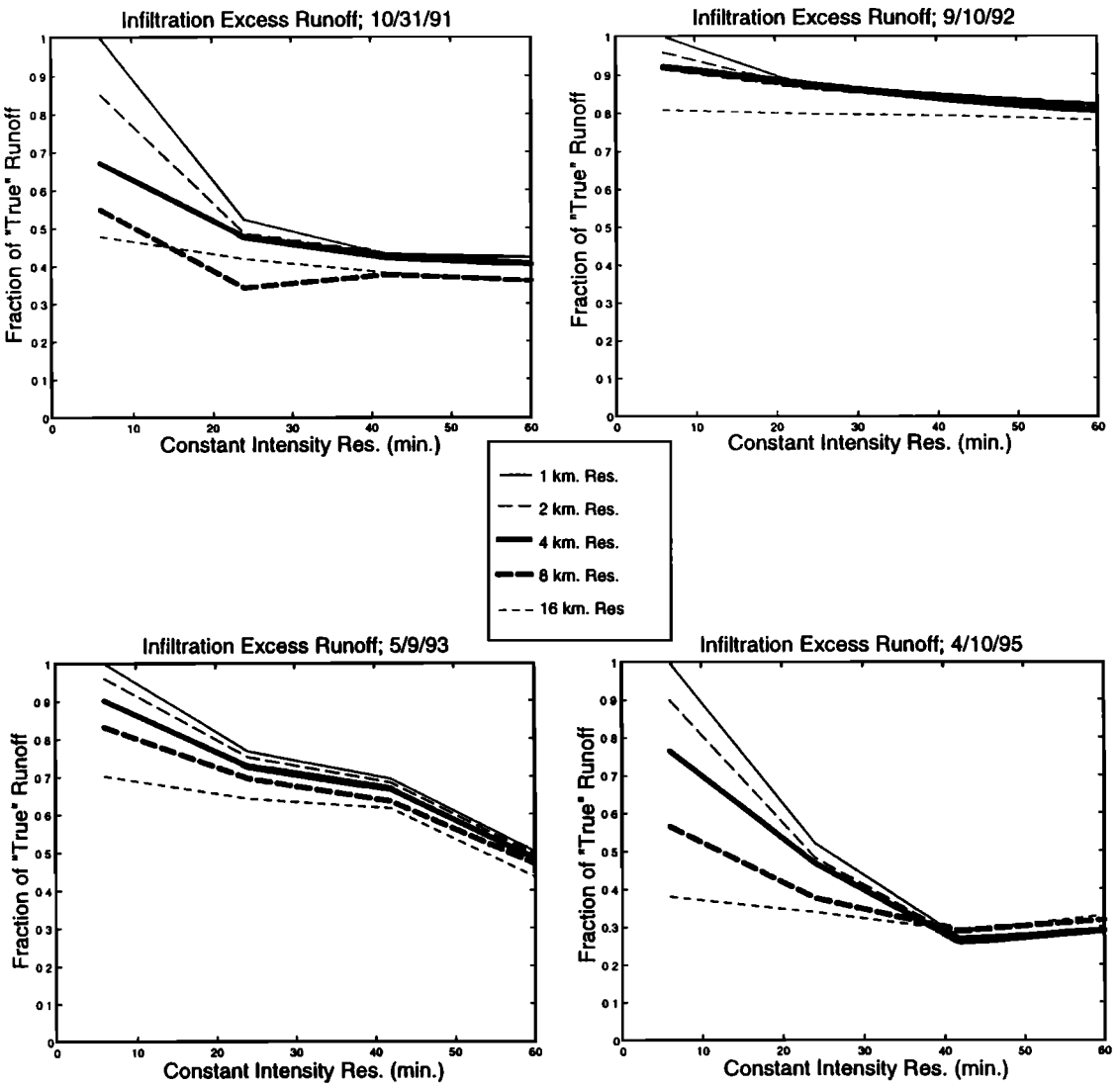

Figure 9. Infiltration-excess runoff sensitivity to temporal and spatial aggregation of normalized precipitation input.

regression statistics also are quite good. However, the r^2 values do drop below 0.75 for the 4-km and 2-km aggregations. Again, this may suggest that these regression equations are more appropriate for predicting runoff reductions due to significant precipitation aggregations. Nevertheless, the predictive ability of all the equations presented is high enough to indicate the potential in this method for correcting errors in runoff simulations.

It should be understood that these equations, in their present form, are not suitable for application in a real-time modeling environment. They require the knowledge of the precipitation intensity distribution after the entire storm, from the finest available resolution data. In addition, these relationships are likely site-specific, suggesting that additional work be performed to verify this and investigate the cause. The main purpose for the development of these equations was as follows. First, they show that runoff response to precipitation resolution is not random, but that it is related to the σ_{MaxInt}. Second, they provide the basis for future research which might focus on a technique which can, in real time, make adjustments to runoff predictions on the basis of the resolution of the precipitation being used and the σ_{MaxInt}.

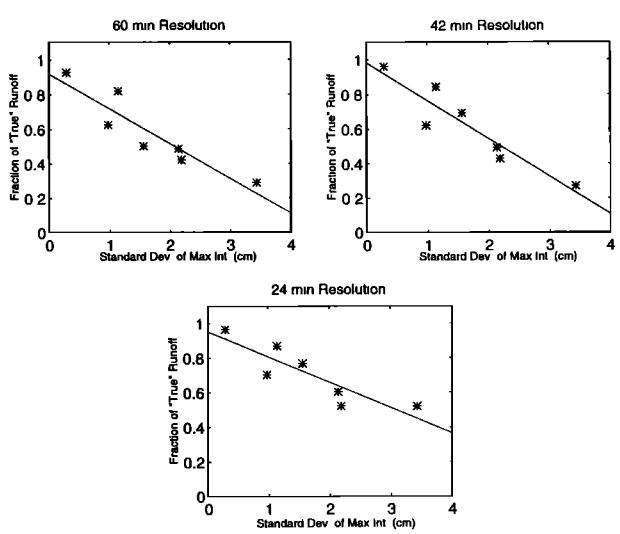

Figure 10. Spatial standard deviation of maximum precipitation intensity versus fraction of true runoff produced; case of temporal aggregation. Each point represents one storm, and the line represents the least squares line.

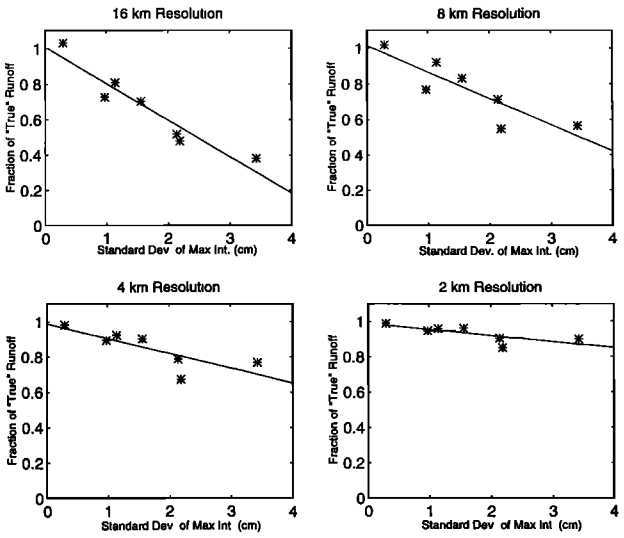

Figure 11. Spatial standard deviation of maximum precipitation intensity versus fraction of true runoff produced; case of spatial aggregation. Each point represents one storm, and the line represents the least squares line.

5. Summary and Conclusions

Several issues related to the use of radar-estimated precipitation in rainfall-runoff modeling have been the focus of this paper. The work was motivated by the rapidly expanding body of NEXRAD Level II data available for use in both research and commercial applications. The increasing availability of NEXRAD Level II data requires that potential users be properly informed regarding effective methods for working with and applying the data to hydrologic applications. The areas emphasized in this report were (1) the effects of errors introduced into the precipitation data by uncertainty in the transformation of reflectivity to rainfall on runoff simulations, (2) how the temporal and spatial resolution of the radar-estimated precipitation data affects runoff simulations, and (3) how the reduction of infiltration-excess runoff resulting from precipitation aggregation can be estimated on the basis of a storm's σ_{MaxInt}. The principal conclusions of the paper are summarized below.

1. Errors in precipitation data resulting from the transformation of reflectivity to rainfall were found to result in equal or larger-sized errors in simulated runoff generation. Errors in simulated infiltration-excess runoff were much larger in magnitude than their respective rainfall errors, while simulated saturation-excess runoff errors were much closer to the size of their respective rainfall errors. Errors in simulated saturation-excess runoff were larger with respect to the rainfall errors when antecedent basin conditions were dry as opposed to wet.

2. Saturation-excess runoff generation was insensitive to the temporal aggregation of precipitation input. Its apparent sensitivity to the spatial aggregation of the precipitation was shown to be an artifact caused by incorrectly "smoothing rainfall volume" either into or out of the watershed. When this change in precipitation volume within the watershed was corrected for, saturation-excess runoff was also insensitive to the spatial aggregation of the precipitation input.

3. Infiltration-excess runoff was very sensitive to the spatial and temporal aggregation of the precipitation input. After correcting for the change in precipitation volume falling within the watershed because of spatial aggregation, results showed the simulated runoff volume decreased as both the spatial and temporal resolution of the precipitation decreased (from 1 to 16 km and 6 to 60 min, respectively). The results also suggest that the reductions in infiltration-excess runoff as a result of temporal aggregation are more significant than those due to spatial aggregation.

4. The sensitivity of infiltration-excess runoff generation to the spatial and temporal resolution of the precipitation input was found to be storm-dependent. Storms having a high degree of spatial variation in the maximum rainfall intensity occurring over the watershed were found to be much more susceptible to gross underestimation of infiltration-excess runoff when the resolution of the precipitation was coarsened. The linear relationships between the reduction of infiltration-excess runoff volume and the σ_{MaxInt}, resulting from different levels of precipitation aggregation, were estimated using simple regression techniques. These relationships may be used to correct the runoff predictions made with aggregated precipitation input, given knowledge of the rainfall characteristics of the storm.

In addition to lending support to current opinion on several important issues, the research presented in this paper has offered several new contributions to the current scientific work on the subject. These new contributions include (1) addressing the issue of radar-estimated precipitation uncertainty in the context of hydrologic applications, (2) explicitly differentiating between the response of infiltration-excess and saturation-excess runoff to uncertainties in precipitation inputs, and (3) showing that the sensitivity of runoff generation to precipitation aggregation may be directly related to a tangible storm

Table 5. Regression Equations for Temporal Aggregation of Precipitation

Statistic	60-Min Resolution	42-Min Resolution	24-Min Resolution
Regression Equation	$y=0.92-0.20x$	$y=0.98-0.22x$	$y=0.95-0.15x$
r^2	0.84	0.87	0.76
Correlation	−0.92	−0.93	−0.87

Here y represents the fraction of "true" runoff, and x represents the spatial standard deviation of maximum precipitation intensity.

Table 6. Regression Equations for Spatial Aggregation of Precipitation

Statistic	16-km Resolution	8-km Resolution	4-km Resolution	2-km Resolution
Regression Equation	$y = 1.0 - 0.21x$	$y = 1.01 - 0.15x$	$y = 0.99 - 0.08x$	$y = 0.99 - 0.03x$
r^2	0.90	0.76	0.63	0.56
Correlation	−0.95	−0.87	−0.79	−0.75

Here y represents the fraction of true runoff and x represents the spatial standard deviation of maximum precipitation intensity.

characteristic. These contributions have the potential to improve the prediction of short-term hydrologic phenomena, such as flash floods. When modeling in regions where saturation-excess is the dominant runoff mechanism, the resolution of the precipitation input may not be very important. If infiltration-excess is the dominant process, then using high-resolution precipitation data will be essential in making an accurate prediction. If high-resolution data (such as 1-km × 6-min) are not available, then proper corrections to the flash-flood predictions could potentially be made on the basis of the resolution of the available data and the σ_{MaxInt}.

It would certainly be of interest to see if the conclusions drawn in this study can be applied to watersheds of different sizes and in other climatic regions. New regions to study might be the midwest and eastern United States. Larger basins, of the order of 500–10,000 km^2, should be studied as well, because that is the basin size of interest to the National Weather Service in their hydrologic modeling applications. The relationships established for the storm-dependent sensitivity to infiltration-excess runoff reduction should surely be tested to see if similar relationships can be established for various other types of catchments.

Acknowledgments. We are grateful for the financial support provided by the Natural and Man-Made Hazard Mitigation Program of the National Science Foundation (BCS-9307411), the Hydrologic Research Laboratory of the National Weather Service (NA57WH0575), and the NASA-EOS project (NAGW2425); NEXRAD data and algorithm descriptions were made available from DeWayne Mitchell of the National Severe Storms Laboratory and Tom Karl of the National Climate Data Center. Data for the Timber Creek watershed were supplied by the U.S. Geological Survey in Texas; computer assistance was provided by James Broermann and Dan Braithwaite.

References

Abbott, M. B., J. C. Bathurst, J. A. Cunge, P. E. O'Connell, and J. Rasmussen, An introduction to the European hydrological system, Systeme Hydrologique Europeen, "SHE," 1, History and philosophy of a physically based, distributed modeling system, *J. Hydrol., 87*, 45–59, 1986.

Ambroise, B., K. Beven, and J. Freer, Toward a generalization of the TOPMODEL concepts: Topographic indices of hydrological similarity, *Water Resour. Res., 32*(7), 2135–2145, 1996.

Battan, L. J., *Radar Observations of the Atmosphere*, 324 pp., Univ. of Chicago Press, Chicago, Ill., 1973.

Becchi, I., E. Caporali, and E. Palmisano, Hydrologic response to radar rainfall maps through a distributed model, *Nat. Hazards, 9*, 95–108, 1994.

Beven, K., and M. J. Kirkby, A physically based variable contributing area model of basin hydrology, *Hydrol. Sci. Bull., 24*, 43–69, 1979.

Beven, K. J., R. Lamb, P. F. Quinn, R. Romanowicz, and J. Freer, TOPMODEL, in *Computer Models of Watershed Hydrology*, edited by V. P. Singh, pp. 627–668, Water Resour. Publ., Fort Collins, Colo., 1995.

Chow, V. T., D. R. Maidment, and L. W. Mays, *Applied Hydrology*, pp. 132–135, McGraw-Hill, New York, 1988.

Cluckie, I. D., Hydrologic applications of weather radar, *World Meteorol. Organ. Bull., 40*(3), 225–231, 1991.

Cochran, R., Soil survey of Grayson County, Texas, 141 pp., Soil Conserv. Serv., U.S. Dep. of Agric., Washington, D. C., 1980.

Collier, C. G., Accuracy of rainfall estimates by radar, I, Calibration by telemetering rain gauges, *J. Hydrol., 83*, 207–223, 1986a.

Collier, C. G., Accuracy of rainfall estimates by radar, II, Comparison with rain gauge network, *J. Hydrol., 83*, 225–235, 1986b.

Collier, C. G., *Applications of Weather Radar Systems: A Guide to Uses of Radar Data in Meteorology and Hydrology*, pp. 1–80, Ellis Horwood, Chichester, England, 1989.

Collier, C. G., and J. M. Knowles, Accuracy of rainfall estimates by radar, III, Application for short-term flood forecasting, *J. Hydrol., 83*, 237–249, 1986.

Collinge, V. K., Weather radar calibration in real time: Prospects for improvement, in *Hydrologic Applications of Weather Radar*, edited by I. D. Cluckie and C. G. Collier, pp. 25–42, Ellis Horwood, Chichester, England, 1991.

Duan, Q., S. Sorooshian, and V. K. Gupta, Effective and efficient global optimization for conceptual rainfall-runoff models, *Water Resour. Res., 28*(4), 1015–1031, 1992.

Dunne, T., and R. D. Black, Partial area contributions to storm runoff in a small New England watershed, *Water Resour. Res., 6*(5), 1296–1311, 1970.

Faures, J. M., D. C. Goodrich, D. A. Woolhiser, and S. Sorooshian, Impact of small-scale spatial rainfall variability on runoff modeling, *J. Hydrol., 173*, 309–326, 1995.

Green, W. H., and G. A. Ampt, Studies on soil physics, 1, The flow of air and water through soils, *J. Agric. Sci., 4*(1), 1–24, 1911.

Horton, R. E., The role of infiltration in the hydrologic cycle, *Eos Trans. AGU, 14*, 446–460, 1933.

Hudlow, M. D., D. R. Greene, P. R. Ahnert, W. F. Krajewski, T. R. Sivaramakrishnan, E. R. Johnson, and M. R. Diass, Proposed off-site precipitation processing system for NEXRAD, in *21st Conference on Radar Meteorology*, pp. 394–403, Am. Meteorol. Soc., Boston, Mass., 1983.

James, W. P., C. G. Robinson, and J. F. Bell, Radar-assisted real-time flood forecasting, *J. Water Resour. Plann. Manage., 119*(1), 32–44, 1993.

Kitchen, M., and R. M. Blackall, Representativeness errors in comparisons between radar and gauge measurements of rainfall, *J. Hydrol., 134*, 13–33, 1992.

Klazura, G. E., and D. A. Imy, A description of the initial set of analysis products available from the NEXRAD WSR-88D system, *Bull. Am. Meteorol. Soc., 74*(7), 1293–1311, 1993.

Kouwen, N., and G. Garland, Resolution considerations in using radar rainfall data for flood forecasting, *Can. J. Civ. Eng., 16*, 279–289, 1989.

Kouwen, N., E. D. Soulis, A. Pietroniro, J. Donald, and R. A. Harrington, Grouped response units for distributed hydrologic modeling, *J. Water Resour. Plann. Manage., 119*(3), 289–305, 1993.

Krajewski, W. F., L. Venkataraman, K. P. Georgakakos, and S. C. Jain, A Monte Carlo study of rainfall sampling effect on a distributed catchment model, *Water Resour. Res., 27*(1), 119–128, 1991.

Loague, K. M., Impact of rainfall and soil hydraulic property information on runoff predictions at the hillslope scale, *Water Resour. Res., 24*(9), 1501–1510, 1988.

Martner, B. E., A field experiment on the calibration of radars with raindrop disdrometers, *J. Appl. Meteorol., 16*, 451–454, 1977.

Mein, R. G., and C. L. Larson, Modeling infiltration during a steady rain, *Water Resour. Res., 9*(1), 384–394, 1973.

Michaud, J. D., and S. Sorooshian, Effect of rainfall-sampling errors on simulations of desert flash floods, *Water Resour. Res., 30*(10), 2765–2775, 1994.

Milly, P. C. D., and P. S. Eagleson, Effects of storm scale on surface runoff volume, *Water Resour. Res., 24*(4), 620–624, 1988.

Mimikou, M. A., and E. A. Baltas, Flood forecasting based on radar rainfall measurements, *J. Water Resour. Plann. Manage., 122*(3), 151–156, 1996.

Numec, J., Water resources systems and climate change, in *Facets of Hydrology*, vol. II, edited by J. C. Rodda, pp. 131–152, John Wiley, New York, 1985.

Obled, C., J. Wendling, and K. Beven, The sensitivity of hydrologic models to spatial rainfall patterns: An evaluation using observed data, *J. Hydrol., 159*, 305–333, 1994.

Ogden, F. L., and P. Y. Julien, Runoff sensitivity to temporal and spatial rainfall variability at runoff plane and small basin scale, *Water Resour. Res., 29*(8), 2589–2597, 1993.

Ogden, F. L., and P. Y. Julien, Runoff model sensitivity to radar rainfall resolution, *J. Hydrol., 158*, 1–18, 1994.

Pessoa, M. L., R. L. Bras, and E. R. Williams, Use of weather radar for flood forecasting in the Sieve River basin: A sensitivity analysis, *J. Appl. Meteorol., 32*(3), 462–475, 1993.

Putnam, L. A., C. R. Cail, R. A. Cochran, W. J. Guckian, L. C. Lovelace, and B. J. Wagner, Soil survey of Cooke County, Texas, 134 pp., Soil Conserv. Serv., U.S. Dep. of Agric., Washington, D. C., 1979.

Quinn, P., K. Beven, P. Chevallier, and O. Planchon, The prediction of

hillslope flow paths for distributed hydrologic modeling using digital terrain models, *Hydrologic Processes*, *5*, 59–79, 1991.

Rawls, W. J., L. R. Ahuja, D. L. Brakensiek, and A. Shirmohammadi, Infiltration and soil water movement, in *Handbook of Hydrology*, edited by D. R. Maidment, pp. 5.1–5.51, McGraw-Hill, New York, 1993.

Schell, G. S., C. A. Madramootoo, G. L. Austin, and R. S. Broughton, Use of radar measured rainfall for hydrologic modeling, *Can. Agric. Eng.*, *34*(1), 41–48, 1992.

Seo, D. J., R. Fulton, J. Breidenbach, D. Miller, and E. Friend, Final report for October 1, 1993 to October 31, 1994, interagency memorandum of understanding among the NEXRAD Program, WSR-88D Operational Support Facility, and the National Weather Service Office of Hydrology Hydrologic Research Laboratory, Hydrol. Res. Lab., Off. of Hydrol., Nl. Weather Serv., Silver Spring, Md., 1995.

Shah, S. M. S., P. E. O'Connell, and J. R. M. Hosking, Modeling the effects of spatial variability in rainfall on catchment response, 2, Experiments with distributed and lumped models, *J. Hydrol.*, *175*, 89–111, 1996.

Smith, J. A., D. J. Seo, M. L. Baeck, and M. D. Hudlow, An intercomparison study of NEXRAD precipitation estimates, *Water Resour. Res.*, *32*(7), 2035–2045, 1996a.

Smith, J. A., M. L. Baeck, M. Steiner, B. Bauer-Messmer, W. Zhao, and A. Tapia, Hydrometeorological assessments of the NEXRAD rainfall algorithms, final report, Dep. of Civ. Eng. and Oper. Res., Princeton Univ., Princeton, N. J., 1996b.

Tees, D., and G. L. Austin, The effects of range on the radar measurement of rainfall, in *Hydrologic Applications of Weather Radar*, edited by I. D. Cluckie and C. G. Collier, pp. 296–304, Ellis Horwood, Chichester, England, 1991.

Winchell, M., H. V. Gupta, and S. Sorooshian, Effects of radar-estimated precipitation uncertainty of different runoff-generation mechanisms, *Tech. Rep. HWR 97-080*, 285 pp., Dep. of Hydrol. and Water Resour., Univ. of Ariz., Tucson, 1997.

Wyss, J., E. R. Williams, and R. L. Bras, Hydrologic modeling of New England river basins using radar rainfall data, *J. Geophys. Res.*, *95*(D3), 2143–2152, 1990.

H. V. Gupta and S. Sorooshian, Department of Hydrology and Water Resources, University of Arizona, Box 210011, Tucson, AZ 85721. (e-mail: hoshin@hwr.arizona.edu)

M. Winchell, Northeast River Forecast Center, National Weather Service, Taunton, MA 02780. (e-mail: Michael.Winchell@noaa.gov)

(Received June 30, 1997; revised June 8, 1998;
accepted June 8, 1998.)